Photocarrier Excitation and Transport in Hyperdoped Planar Silicon Devices.

Journal:	*2011 MRS Spring Meeting*
Manuscript ID:	MRSS11-1321-A08-16.R1
Manuscript Type:	Symposium A
Date Submitted by the Author:	n/a
Complete List of Authors:	Persans, Peter; Rensselaer Polytechnic Institute, Physics Berry, Nathaniel; Rensselaer Polytechnic Institute, Physics Recht, Daniel; Harvard University, Engineering and Applied Sciences Hutchinson, David; Rensselaer Polytechnic Institute Said, Aurore; Harvard University, Engineering and Applied Sciences Warrender, Jeffrey; Benet Laboratories - ARDEC Peterson, Hannah; Rensselaer Polytechnic Institute DiFranzo, Anthony; Rensselaer Polytechnic Institute McGahan, Christina; Rensselaer Polytechnic Institute Clark, Jessica; Rensselaer Polytechnic Institute Cunningham, William; Rensselaer Polytechnic Institute Aziz, Michael; Harvard University, Engineering and Applied Sciences
Keywords:	Si, photoconductivity, laser annealing

Photocarrier Excitation and Transport in Hyperdoped Planar Silicon Devices

Peter D. Persans[1], Nathaniel E. Berry[1], Daniel Recht[2], David Hutchinson[1], Aurore J. Said[2], Jeffrey M. Warrender[3], Hannah Peterson[1,3], Anthony DiFranzo[1], Christina McGahan[1], Jessica Clark[1], Will Cunningham[1], and Michael J. Aziz[2]

[1]Rensselaer Polytechnic Institute, 110 8th Street, Troy NY 12180
[2] Harvard, School of Engineering and Applied Science, 29 Oxford Street, Cambridge, MA 02138
[3]US Army – ARDEC, Benet Laboratories, Watervliet, NY 12189

ABSTRACT

We report an experimental study of photocarrier lifetime, transport, and excitation spectra in silicon-on-insulator doped with sulfur far above thermodynamic saturation. The spectral dependence of photocurrent in coplanar structures is consistent with photocarrier generation throughout the hyperdoped and undoped sub-layers, limited by collection of holes transported along the undoped layer. Holes photoexcited in the hyperdoped layer are able to diffuse to the undoped layer, implying $(\mu\tau)_h \sim 5\times10^{-9}$ cm^2/V. Although high absorptance of hyperdoped silicon is observed from 1200 to 2000 nm in transmission experiments, the number of collected electrons per absorbed photon is 10^{-4} of the above-bandgap response of the device, consistent with $(\mu\tau)_e < 1\times10^{-7}$ cm^2/V.

INTRODUCTION

Pulsed laser irradiation enables the production semiconductors that have compositions not readily attainable with other methods and that exhibit interesting and potentially useful optical properties[1, 2]. Recently, optically smooth sulfur-supersaturated crystalline silicon has been fabricated in thin film form using ion implantation followed by nanosecond pulsed laser melting [3]. This new material exhibits an unexpectedly high sub-bandgap absorption coefficient [2, 3]. The nature of the transitions that give rise to this absorption has not yet been determined, however free carrier absorption has been ruled out. The present work is an attempt to elucidate the excitation and photoconduction mechanisms in hyperdoped silicon devices.

EXPERIMENT

Hyperdoped layers were prepared by implantation of sulfur into a thin crystalline silicon-on-insulator (SOI) layer, followed by pulsed laser melting to rapidly recrystallize the implanted layer while retaining a high dopant concentration [3]. For the current study, the SOI layer was 260 nm thick with a 1000 nm oxide. The peak implant density of ~10^{20} cm^{-3} is about 110 nm deep. After laser melting of the top 200 nm, the peak S density is about 2.5x10^{19} cm^{-3}. The back 50 nm of the SOI layer is not melted in order to act as a seed layer for crystalline regrowth. Au surface contacts for coplanar measurements were evaporated with a 0.8 mm gap.

The optical absorption coefficient for a hyperdoped layer prepared by implantation of 10^{15} S ions per cm^2 followed by pulsed laser melting is plotted against wavelength in Fig. 1 [4, 5]. Dilute sulfur doping leads to donor impurity levels 0.3 eV below the conduction band [6, 7]. It has been proposed that hyper-doping with S leads to an impurity band [3]. About 10% of S impurities lead to carriers in the conduction band [8].

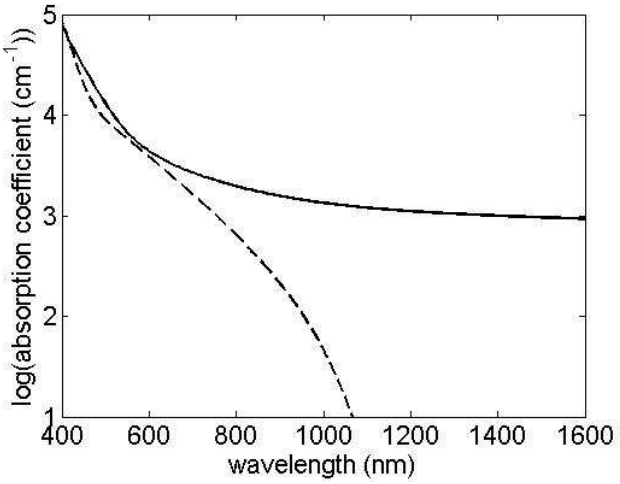

Figure 1. Optical absorption coefficient plotted as a function of wavelength for undoped Si (dashed line) and chalcogen hyperdoped Si (solid line). Sulfur implantation dose for the hyperdoped sample is $1x10^{15}cm^{-2}$. (from Pan et al. [5])

Room temperature dark current-voltage curves were ohmic and n-type, yielding a sample resistance of 1440 ohms and layer conductivity of 20 $\Omega^{-1}cm^{-1}$, consistent with carrier density of ~10^{19} cm^{-3} [9, 10]. Electron Hall mobility of ~ 50 cm^2/Vs has been reported in similar materials [7]. Photocurrent under typical illumination levels is orders of magnitude smaller than dark current, so steady state photocurrent was detected using chopping and lock-in techniques [11]. Transient photocurrent was measured using a 5 nanosecond nitrogen laser pumped dye laser at 650 nm and oscilloscope.

RESULTS AND DISCUSSION

Photocurrent magnitude was nearly linear in voltage for applied voltages less than 0.5 V and displayed saturation for voltage greater than ~1.2V (Fig. 2). For a given applied voltage, cw photocurrent was linear with intensity. Transient photocurrent measurements, extrapolated to zero applied field, yielded exponential current decay with decay lifetime of ~40 μs. We note that this is a surprisingly large value for heavily doped material – typical free carrier lifetimes for heavily doped material are less than 10 ns [12]. Saturation of photocurrent with increasing voltage occurs in metal-semiconductor-metal devices either when primary photocarriers are not re-injected or when the minority carrier drift length $L_{drift} = \mu\tau E$ exceeds the length of the sample [11]. Reinjection of electrons is likely, due to the ohmic contacts, so photocurrent is likely limited by minority carrier extraction. Our observed saturation field of ~20 V/cm for a sample width of 0.8 mm yields $\mu\tau = 3\times10^{-3}$ cm^2/V for minority carriers. Using the decay lifetime of 40 μs, we find a drift mobility of ~75 cm^2/Vs.

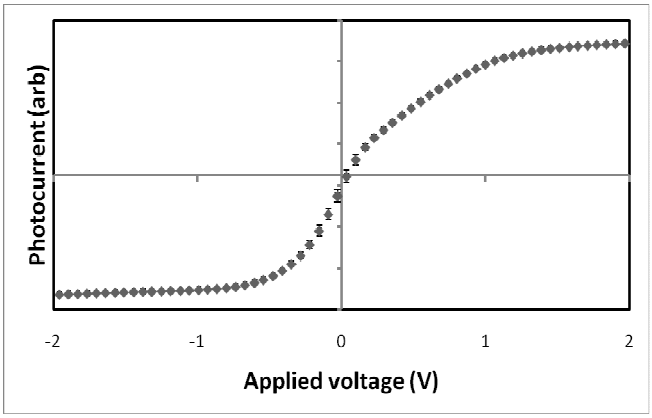

Figure 2. Photocurrent as a function of voltage applied across the sample. Excitation wavelength was 660 nm.

The combination of high drift mobility and long decay lifetime is not expected for photocarrier transport in hyperdoped Si – long decay lifetime implies carrier trapping and trapping decreases drift mobility [13]. We therefore propose a photocarrier model in which electron and hole photocarriers are quickly separated into different layers of the sample. The structure of the sample, sketched in Figure 3, provides a mechanism. The doping profile is abrupt, leaving the bottom ~50 nm seed layer with much less active sulfur [3, 14]. This leads to a profile in which photoexcited holes can diffuse or drift a short distance to the undoped seed layer and electrons remain in the hyperdoped layer, as shown in case A in the sketch. If the $(\mu\tau)$ product for holes in the seed layer exceeds that of electrons in the hyperdoped layer, then photocurrent saturation occurs when holes are swept from the bottom layer, recombining with electrons in the external circuit.

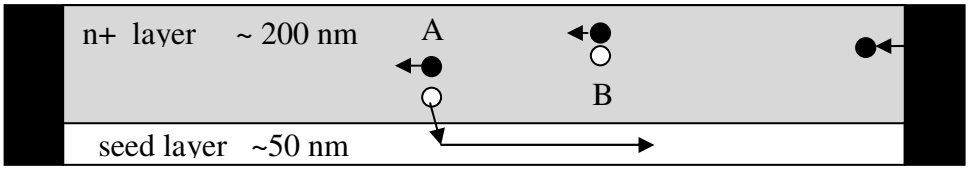

Figure 3. A schematic side-view of the silicon-on-insulator layer showing the proposed motion of photogenerated electrons (black) and holes (white). The doped layer is about 200 nm thick and the undoped seed layer is about 50 nm thick. Free holes generated in the doped layer leave the doped layer and travel laterally in the seed layer (case A). Electrons and trapped holes remain in the doped layer (case B). The sketch is not to scale. The aspect ratio of thickness to length is ~3×10^{-3}.

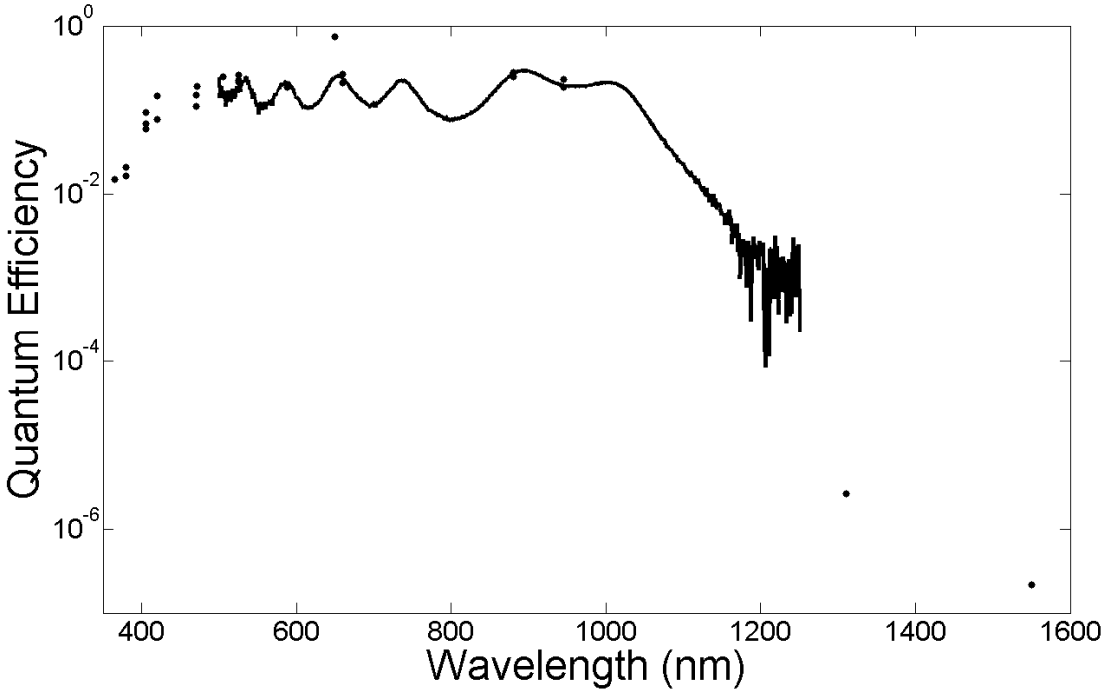

Figure 4. Spectral response as a function of wavelength. Solid line is collected with a scanned monochromator with a tungsten-halide lamp source. Points are collected with LED and laser sources. The two data points at 1310 and 1550 nm are upper bounds on the signal.

The photocurrent spectrum, normalized to display electronic charge collected per incident photon (external quantum efficiency), is plotted in Fig. 4 for wavelength from 365 nm to 1550 nm. External quantum efficiency for applied voltage of 1 V is 0.1 to 0.3 electrons per incident photon for wavelength from 600 to 1000 nm. Absorption interference fringes are expected and observed due to the multilayer SOI structure. The external quantum efficiency decreases rapidly for wavelengths above 1100 nm and drops to less than 10^{-7} at 1550 nm. The external quantum efficiency also drops for wavelengths shorter than 500 nm. The continuous line was collected using a monochromator system, while the individual points were collected using LEDs and lasers.

The absence of response beyond 1200 nm further constrains the photoconduction models. Collection efficiency for sub-bandgap excitation is at least 10^4 times smaller than would be expected if the photocarrier were the same for above and below gap excitation. Sub-bandgap absorption should result in a free electron and a trapped hole in an impurity state in the hyperdoped layer (illustrated as case B in the sketch in Fig. 3). The electron collection efficiency would then be $L_{drift} / L = \mu_n \tau_n V / L^2$, where L is the distance between contacts. Absorptance in the hyperdoped layer at 1550 nm is about A=10^{-2}, so the observed collection efficiency of $< 3\text{x}10^{-7}$ implies $\mu_n \tau_n < 2\text{x}10^{-7}$ cm^2/V in the hyperdoped layer.

The free electron lifetime in the hyperdoped layer is expected to be shorter than 1 ns because the equilibrium density of holes (in impurity states) is high (~10^{18} cm^{-3}). Assuming

reasonable values from the literature of free carrier mobility of 50 cm^2/Vs [7] and lifetime of $\tau < 10^{-9}$ s [10], yields an expected upper bound of $(\mu\tau)_e < 10^{-7}$ cm^2/V.

Photocurrent response at 365 nm, where absorption is entirely in the hyperdoped material, is 10^5 times greater than in the infrared. This is explained if holes generated at the top surface can diffuse or drift about 150 nm to the undoped layer. Assuming diffusion-limited transport, this yields an estimate of $(\mu\tau)_h \cong 5\times10^{-9}$ cm^2/V for holes in the hyperdoped layer.

CONCLUSIONS

Experimental measurement of coplanar photoresponse in a 260 nm thick silicon on insulator layer sets limits on photocarrier excitation, recombination, and transport. We propose that:

i) Electron-hole pairs excited with above bandgap radiation separate into hyperdoped and seed layers, leading to longer than expected lifetimes.
ii) The n+ contact-metal band structure allows holes to escape easily, but they cannot be re-injected. (This leads to saturation.)
iii) Electron-hole pairs excited with sub-bandgap radiation leave holes trapped on the impurity states in the hyperdoped layer, which provide sites for rapid recombination.
iv) The fall off of response for wavelengths shorter than 400 nm is consistent with the short lifetime and diffusion length proposed for holes and electrons in the hyperdoped layer.

These model assumptions lead to limits on the free carrier mobility-lifetime product for carriers in S-hyperdoped material of $\mu_n\tau_n < 2\text{x}10^{-7}$ cm^2/V for electrons and $\mu_p\tau_p \approx 5\text{x}10^{-9}$ cm^2/V for holes.

ACKNOWLEDGMENTS

This work is supported in part by the Army Research Office under contract No. W911NF0910470, US Army ARDEC under contract No. W15QKN-07-P-0092, and by the NSF REU programs at Harvard and at Rensselaer. Prepublication optical data were provided by Athena Pan (Brandeis University). Prepublication carrier density and majority carrier mobility data were supplied by Mark Winkler (Harvard University and MIT). We have benefitted from discussions with James Carey of SiOnyx Inc., Eric Schiff (Syracuse University), and Tonio Buonassisi (MIT).

REFERENCES

1. J.E. Carey, C.H. Crouch, M.Y. Shen, and E. Mazur, *Visible and near-infrared responsivity of femtosecond-laser microstructured silicon photodiodes.* Optics Letters, 2005. **30**(14): p. 1773-1775.
2. C.H. Crouch, J.E. Carey, J.M. Warrender, M.J. Aziz, E. Mazur, and F.Y. Genin, *Comparison of structure and properties of femtosecond and nanosecond laser structured silicon.* Appl. Phys. Lett., 2004. **84**: p. 1850.
3. T.G. Kim, J.M. Warrender, and M.J. Aziz, *Strong sub-band-gap infrared absorption in silicon supersaturated with sulfur.* Appl. Phys. Lett., 2006(241902).

4. S.H.A. Pan, *Enhanced Visible Absorption of Ion Implanted and Pulse Laser Melted Si Supersaturated with Chalcogens*. 2010, Brandeis University.
5. S.H. Pan, D. Recht, S. Charnvanichborikarn, J. Williams, S., and M.J. Aziz, *Enhanced visible and near-infrared optical absorption in silicon supersaturated with chalcogens.* Appl. Phys. Lett., 2011. **98**: p. 121913.
6. H.G. Grimmeiss and E. Janzen, in *Handbook on Semiconductors*, T.S. Moss and S. Mahajan, Editors. 1994, Elsevier: Amsterdam.
7. M. Winkler, *Non-Equilibrium Chalcogen Concentrations in Silicon: Physical Structure, Electronic Transport, and Photovoltaic Potential*, in *Physics*. 2010, Harvard: Cambridge, MA.
8. M. Winkler, D. Recht, M.-J. Sher, A.J. Said, E. Mazur, and M.J. Aziz, *Insulator to Metal Transition in Sulfur Doped Silicon.* Phys. Rev. Lett., 2011. **106**: p. 178701.
9. H.F. Wolf, *Semiconductors*. 1971, New York: Wiley- Interscience.
10. S.M. Sze, *Physics of Semiconductor Devices*. 1981, New York: Wiley.
11. S.M. Ryvkin, *Photoelectric effects in semiconductors*. 1964, New York: Consultants Bureau.
12. M.S. Tyagi and R. VanOverstraeten, *Minority carrier recombination in heavily doped silicon.* Solid State Electronics, 1983. **26**: p. 577-598.
13. E.A. Schiff, *Transit-time measurements of charge carriers in disordered silicons: Amorphous, microcrystalline and porous.* Phil. Mag., 2009. **89**: p. 2505-2518.
14. M. Tabbal, T.G. Kim, J.M. Warrender, M.J. Aziz, B.L. Cardozo, and R.S. Goldman, *Formation of single crystal sulfur supersaturated silicon based junctions by pulsed laser annealing.* J. Vac. Sci. Technol. B, 2007. **25**: p. 1847.